Standard Model $H \to ZZ^*$ polarization measurement and $WZ\gamma$ observation at CMS

Leyun Gao (on behalf of the CMS Collaboration)

Peking University

IAS Program on Fundamental Physics (FP 2026) Junarary 12, 2025

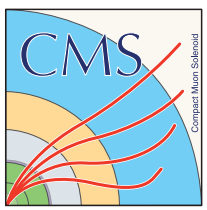

Overview: precision as a path to new physics

The LHC probes both the Standard Model (SM) and physics beyond it:

- Direct searches push the scale of new physics to higher energies.
- Precision measurements provide complementary sensitivity.
- Beyond new particles, deviations from the SM may appear in e.g.:
  - polarization and spin correlations
  - rare multi-boson final states
  - energy-growing amplitudes
- Effective Field Theory (EFT) provides a unified framework to interpret such effects.

Two case studies in this talk:

- Higgs: polarization and entanglement in $H \to ZZ^*$
- Multi-boson production: rare $WZ\gamma$ processes and anomalous gauge couplings

Documentation

- $H \to ZZ^*$ polarization measurement:

CMS-PAS-HIG-25-011

Available on the CERN CDS information server **CMS PAS HIG-25-011**

CMS Physics Analysis Summary

Contact: cms-pag-conveners-higgs@cern.ch 2025/11/27

Study of spin correlations in Higgs boson decays to four leptons at CMS

The CMS Collaboration

Abstract

Kinematic distributions in Higgs boson decay to four leptons $H \to 4\ell$ are studied using matrix element techniques, optimizing sensitivity to the tensor structure of Higgs boson interactions and spin correlations in the decay process. The data were collected by the CMS experiment at the LHC, corresponding to integrated luminosities of 138 and 62 fb^{-1} at proton-proton center of mass energies of 13 and 13.6 TeV, respectively, covering the 2016–2018 and 2022–2023 data-taking periods. A simultaneous measurement of eight Higgs boson couplings to electroweak vector bosons is carried out within the frameworks of anomalous couplings and effective field theory. Under the assumption of *CP* symmetry conservation, the polarization density matrix in the $H \to ZZ$ decay is measured, and a search for *CP* violation in the polarization of the Z bosons is conducted. Quantum mechanical interference is tested through the permutation of identical leptons. Implications regarding quantum entanglement and the violation of a Bell-type inequality are discussed.

- $WZ\gamma$ observation:

Phys. Rev. D 112 (2025), 012009

PHYSICAL REVIEW D **112,** 012009 (2025)

Observation of $WZ\gamma$ production and constraints on new physics scenarios in proton-proton collisions at $\sqrt{s} = 13$ TeV

V. Chekhovsky *et al.*[*]
(CMS Collaboration)

(Received 27 March 2025; accepted 27 May 2025; published 15 July 2025)

A measurement of the $WZ\gamma$ triboson production cross section is presented. The analysis is based on a data sample of proton-proton collisions at a center-of-mass energy of $\sqrt{s} = 13$ TeV recorded with the CMS detector at the LHC, corresponding to an integrated luminosity of 138 fb^{-1}. The analysis focuses on the final state with three charged leptons, $\ell^{\pm}\nu\ell'^{+}\ell'^{-}$, where $\ell' = e$ or μ, accompanied by an additional photon. The observed (expected) significance of the $WZ\gamma$ signal is 5.4 (3.8) standard deviations. The cross section is measured in a fiducial region, where events with an ℓ originating from a tau lepton decay are excluded, to be 5.48 ± 1.11 fb, which is compatible with the prediction of 3.69 ± 0.24 fb at next-to-leading order in quantum chromodynamics. Exclusion limits are set on anomalous quartic gauge couplings and on the production cross sections of massive axionlike particles.

DOI: 10.1103/cm24-665b

I. INTRODUCTION

The discovery of the Higgs boson at the CERN LHC [1–3] experimentally confirmed the principle of electroweak (EW) symmetry breaking [4–6] and the mechanism through which the W and Z bosons acquire mass. Following that, many studies have been conducted on physics scenarios beyond the standard model (BSM) as well as the precision measurement of known standard model (SM) processes. Most of those studies show good agreement with the SM [7–11], motivating BSM searches in previously unexplored event topologies as well as precision measurements of rare SM processes. The CMS Collaboration has observed the combined production of three massive gauge bosons at $\sqrt{s} = 13$ TeV [12]. Recently, also at 13 TeV, $W\gamma\gamma$ production has been observed by the ATLAS and CMS Collaborations [13,14], and $Z\gamma\gamma$ and $WW\gamma$ production has been observed by CMS [14,15]. An observation of $WZ\gamma$ production in 13 TeV proton-proton (pp) collisions has been reported by the ATLAS Collaboration [16].

Multiboson production processes are sensitive to contributions with triple gauge couplings (TGCs) and quartic gauge couplings (QGCs). Many BSM models alter these couplings between the gauge bosons. These contributions can be parametrized through anomalous couplings, which can be described in an effective field theory [17]. As one example, the $WZ\gamma$ process is sensitive to potential anomalous TGCs and QGCs (aQGCs). In addition, the study of $WZ\gamma$ production can be used to search for an axion-like particle (ALP) [18–23]. The axion is a hypothesized pseudoscalar particle, predicted by the Peccei-Quinn [24,25] solution of the strong charge-conjugation-parity problem in quantum chromodynamics (QCD). The axion is also a candidate for dark matter. At the LHC, certain types of photophobic ALPs, denoted a, can be explored in $Z\gamma$ final states [26]. Figure 1 shows representative Feynman diagrams at leading order (LO) for $WZ\gamma$ production through QGCs, TGCs, multiperipheral interaction, and an ALP, from left to right, respectively.

This paper reports the measurement of the $WZ\gamma$ production fiducial cross section in pp collisions at a center-of-mass energy of 13 TeV corresponding to an integrated luminosity of 138 fb^{-1}, recorded with the CMS detector at the LHC. Both the W and the Z bosons are identified via their leptonic decays. Limits on aQGCs, as well as constraints on the ALP model, are also presented. Tabulated results are provided in HEPData [27].

II. THE CMS DETECTOR

The central feature of the CMS [28] apparatus is a superconducting solenoid of 6 m internal diameter, providing a magnetic field of 3.8 T. A silicon pixel and strip tracker, a lead tungstate crystal electromagnetic calorimeter (ECAL), and a brass and scintillator hadron calorimeter (HCAL), each composed of a barrel and two end cap sections, reside within the solenoid volume. Forward calorimeters extend the coverage provided by the barrel

[*]Full author list given at the end of the article.

$H \to ZZ^*$ polarization measurement

$H \to ZZ^* \to 4\ell$ as an excellent probe of polarization and entanglement

Advantages:

- $H \to ZZ^* \to 4\ell$ is a golden channel for precision studies of Higgs properties.
- The 4ℓ final state is experimentally clean, with very small QCD background.

Methodology:

- The full polarization density matrix of the ZZ system can be directly reconstructed from lepton flavors and four-momenta using quantum tomography (detailed in J. A. Aguilar-Saavedra's paper and Andrew Levin's talk on Jan 15).
- Alternatively, properties of interest, such as the SM $H \to ZZ^*$ polarization fractions, can be extracted via template fits (covered in this talk).
- The measurement is also sensitive to quantum entanglement and tests of Bell inequalities.

Definition of reference frame and angles

1. Boost to the Higgs boson rest frame.
2. Rotate to a right-handed coordinate system where the z-axis points along the direction of Z_1 (the Z boson with mass closer to the nominal Z mass), and the x-axis lies along the component of the beamline orthogonal to the z-axis.
3. Boost to the rest frames of Z_1 and Z_2 (where Z_2 is the Z boson with mass farther from the nominal Z mass).

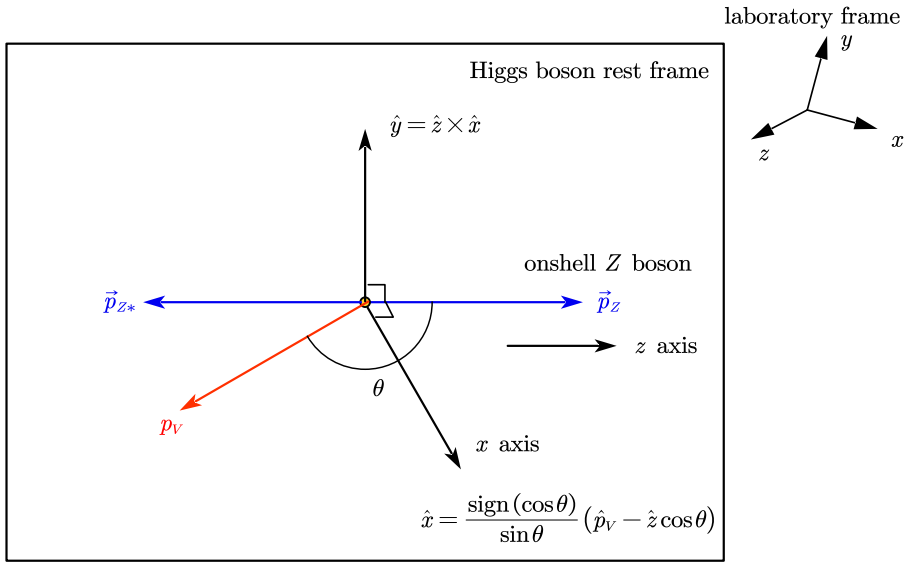

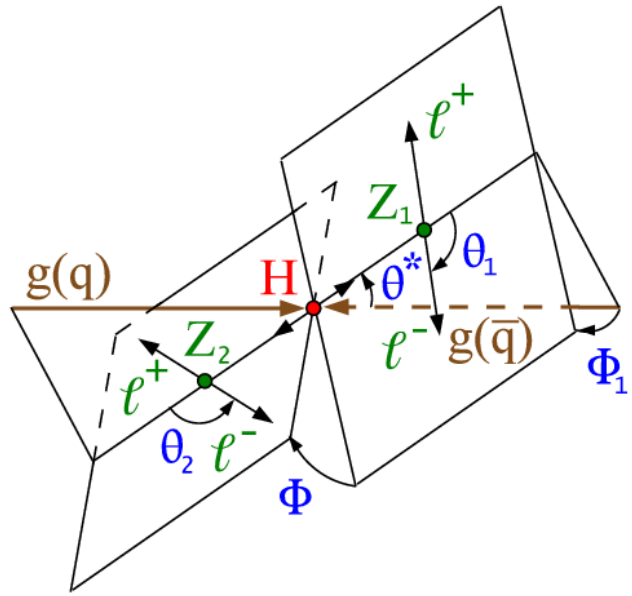

$H \to ZZ^*$ polarization modeling

- SM $H \to ZZ^* \to 4\ell$ decays are simulated with JHUGen.
- MELA provides matrix-element-based likelihoods for various signal polarization modes (JHUGen, for SM/LL/TT/interference) and background (MCFM).
- Interference between the two pairing schemes in same-flavor 4ℓ final states (as an identical lepton effect) is considered.
- SM events are reweighted using likelihood ratios to model the intended ZZ polarization states (LL/TT/interference).

$$A_{00} = -\frac{m_H^2}{v}\left(a_1\sqrt{1+x} + a_2\frac{m_1 m_2}{m_H^2}x\right),\ A_{\pm\pm} = \frac{m_H^2}{v}\left(a_1 \pm \mathrm{i}a_3\frac{m_1 m_2}{m_H^2}\sqrt{x}\right),$$

$$a_1 = g_1^{(0)}\frac{m_Z^2}{m_H^2} + \frac{s}{m_H^2}\left(2g_2^{(0)} + g_3^{(0)}\frac{s}{\Lambda^2}\right),\ a_2 = -\left(2g_2^{(0)} + g_3^{(0)}\frac{s}{\Lambda^2}\right),\ a_3 = -2g_4^{(0)},$$

$$x = \left(\frac{m_H^2 - m_1^2 - m_2^2}{2m_1 m_2}\right)^2 - 1,\ s = \frac{m_H^2 - m_1^2 - m_2^2}{2}.$$

(for HVV) Red: helicity amplitudes; Cyan: tunable couplings in MELA.

Event reconstruction and selection

- Trigger: $\ell\ell$, additionally ℓ and $\ell\ell\ell$. Efficiency $> 99\%$ for selected signal.
- Object reconstruction: CMS particle-flow candidates $\rightarrow$ electrons, muons, photons, and hadrons $\rightarrow$ jets and isolation variables.
- Electrons (muons) with $p_{\mathrm{T}} > 7\,(5)$ GeV and $|\eta| < 2.5\,(2.4)$.
- Primary vertex: highest $\sum p_{\mathrm{T}}^2$ of physics objects; jets clustered with anti-k_T $R = 0.4$, $p_{\mathrm{T}} > 30$ GeV, $|\eta| < 4.7$, $\Delta R(\ell/\gamma, \mathrm{jet}) > 0.4$.
- Lepton selection: $|SIP| < 4$ to ensure consistency with primary vertex; isolation applied to reduce nonprompt backgrounds.
- Channels: $H \to 4e, 4\mu, 2e2\mu$; at least two leptons with $p_{\mathrm{T}} > 10$ GeV and one with $p_{\mathrm{T}} > 20$ GeV.
- Z candidates: $12 < m_{\ell^+\ell^-} < 120$ GeV, at least one > 40 GeV; analysis region $105 < m_{4\ell} < 140$ GeV.

Event reconstruction and selection

Production mode	$2e2\mu$	$4e$	4μ	Total
Signal expected	159.3	59.6	133.0	351.9
$q\bar{q} \to 4\ell$ bkg	144.5	47.3	133.8	325.6
$gg \to 4\ell$ bkg	11.9	6.0	14.6	32.5
EW bkg	5.8	2.1	3.3	11.2
Z+X bkg	70.4	16.3	61.3	148.0
Total expected	391.9	131.3	346.0	869.2
Total observed	423	141	333	897

Table: Expected signal and background yields and observed events for 2016–2023 ($200\ \mathrm{fb}^{-1}$).

We are actively working on 2024 data ($109\ \mathrm{fb}^{-1}$).

Kinematic distributions ($D_{\text{bkg}} > 0.6$ except for $m_{4\ell}$ for visualization)

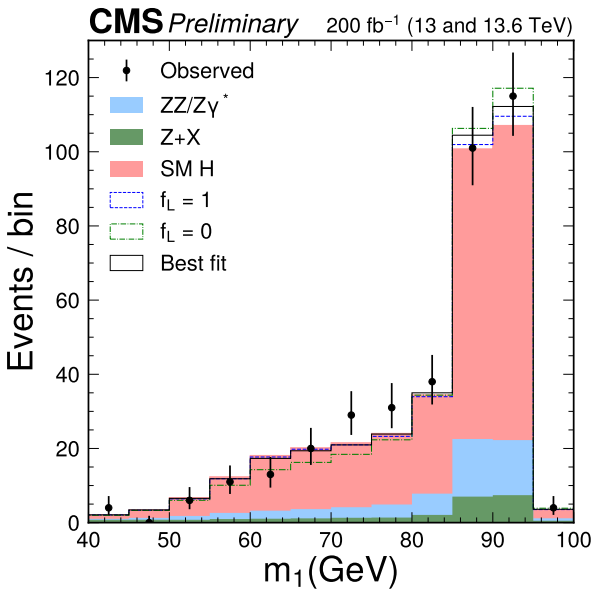

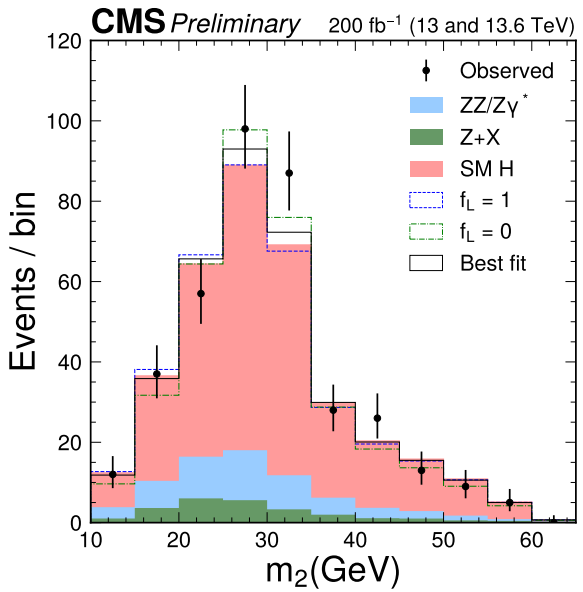

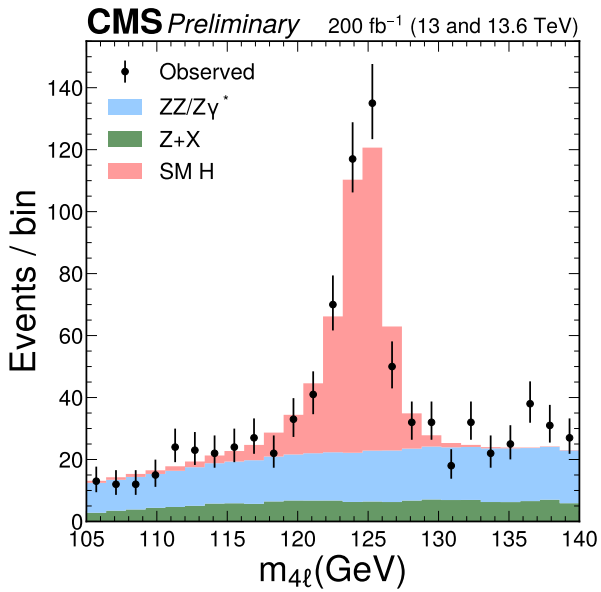

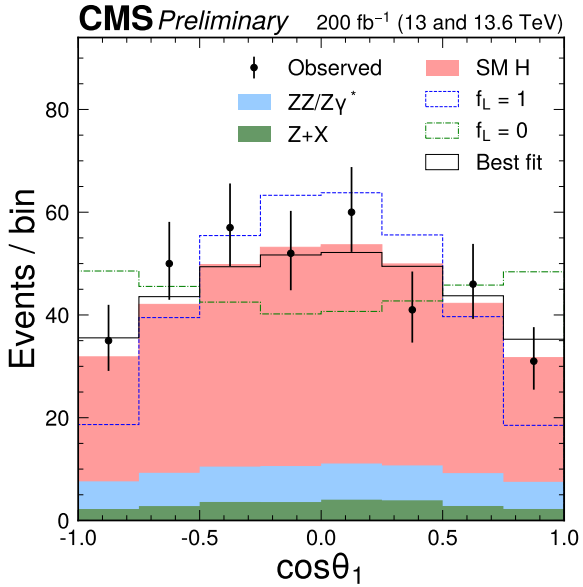

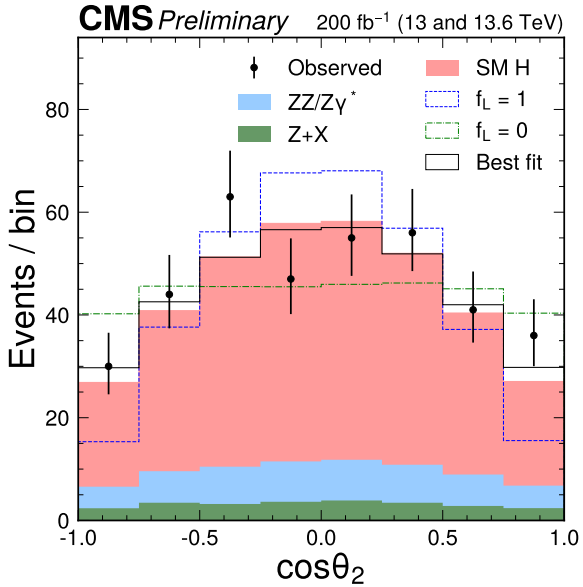

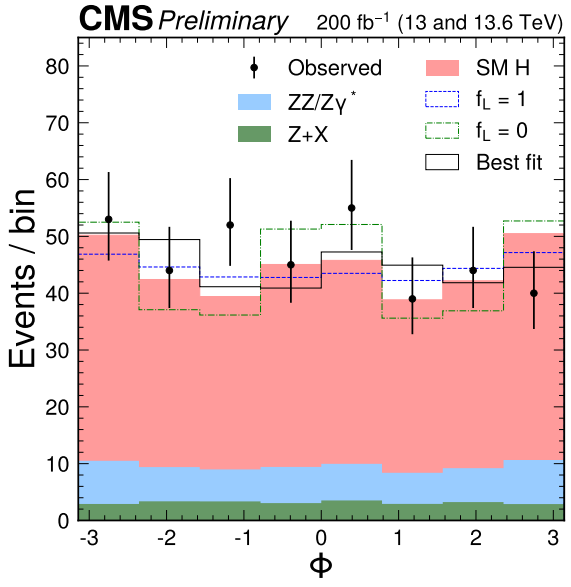

Template fit for polarization fractions

- Polarization fractions f_L and $f_\perp$ are extracted.
- A 4D binned likelihood scan in $(D_{\text{bkg}}, \cos\theta_1, \cos\theta_2, \Phi)$ is performed.
- Mass observables (m_1, m_2) are integrated out and constrained to be polarization-independent.
- The model reproduces the SM expectation ($f_L = 0.61$, $f_\perp = 0$).

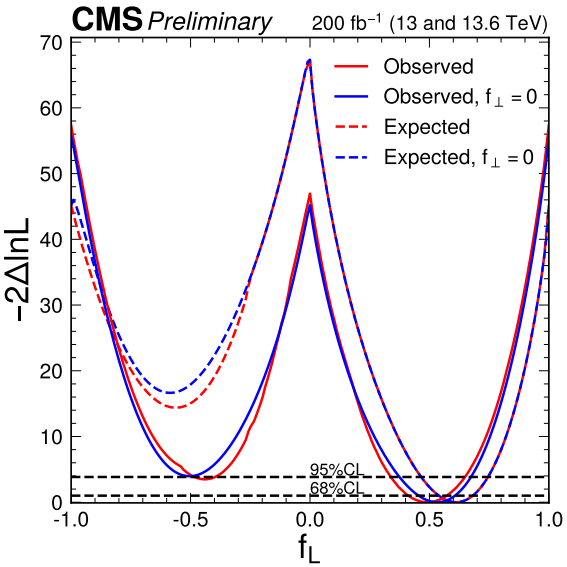

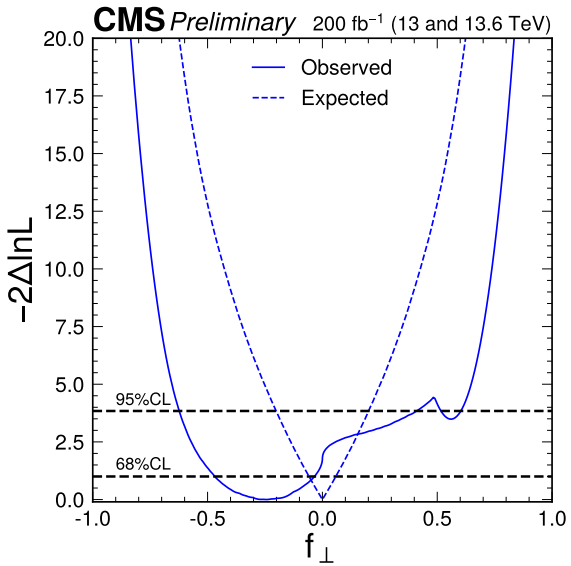

Parameter	Observed	Expected
f_L	$0.49^{+0.08}_{-0.07}$	0.61 ± 0.07
$f_\perp$	$0.25^{+0.21}_{-0.22}$	0.00 ± 0.06

$> 5\,\sigma$ for $f_L \neq 1$
$\Rightarrow$ quantum entanglement

Deviation from SM interpreted as EFT constraints (not shown here)

Figure: Observed (solid) and expected (dashed) likelihood scans of f_L (left) and $f_\perp$ (right), with the SM expectation $f_L = 0.61$ and $f_\perp = 0$.

$WZ\gamma$ observation

Introduction

- The Higgs discovery at the LHC confirmed electroweak symmetry breaking (EWSB) and the Higgs mechanism giving mass to W and Z bosons.
- Precision studies of SM processes show good agreement with theory, motivating searches for rare processes and BSM physics.
- $WZ\gamma$ production at $13\ \mathrm{TeV}$ probes anomalous triple/quartic gauge couplings (aTGCs/aQGCs) and axion-like particles (ALPs), potential dark matter candidates.
- Recently, CMS measured the $WZ\gamma$ fiducial cross section using leptonic W and Z decays with $138\ \mathrm{fb}^{-1}$ at $13\ \mathrm{TeV}$, setting limits on aQGCs and ALPs.

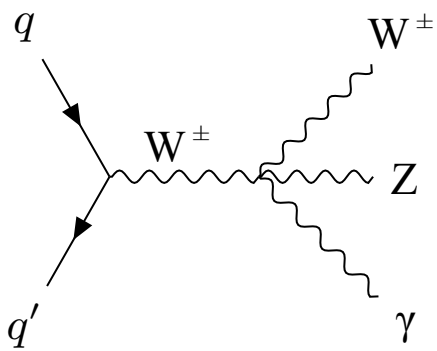

(a) QGC

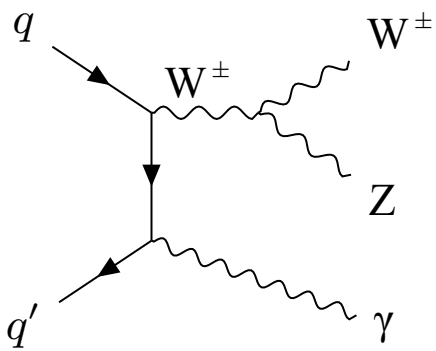

(b) TGC

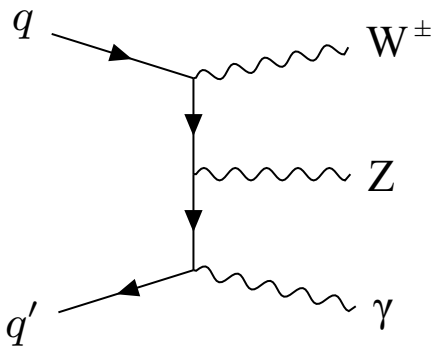

(c) multiperipheral

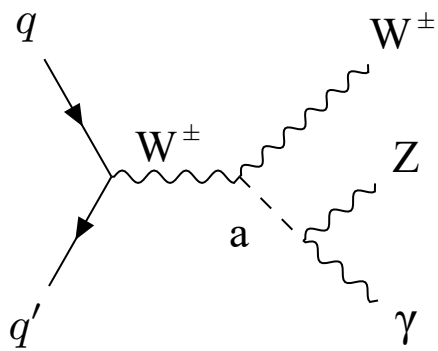

(d) ALP

Signal and background modeling

- Signal: inclusive $\ell\nu\ell^+\ell^-\gamma$ ($\ell = e, \mu$) simulated with MadGraph5_aMC@NLO v2.6.5 at NLO; ℓ from τ decays included; $m_{\ell^+\ell^-} > 4$ GeV.
- Backgrounds:
  - Top quark: $t\bar{t}W/t\bar{t}\gamma$ (NLO, FxFx), $t\bar{t}Z/tZq$ (NLO), tW (POWHEG v2.0)
  - $V\gamma$ ($V = W, Z$) at NLO (FxFx)
  - VV: WZ/ZZ (POWHEG), $gg \to ZZ$ (MCFM LO)
  - VVV: WWW, WWZ, WZZ, ZZZ, $ZZ\gamma$, $Z\gamma\gamma$ (NLO)
- aQGC and ALP events simulated with MadGraph5_aMC@NLO; matrix-element reweighting applied for anomalous couplings.
- Parton showering and hadronization with Pythia using tune CP5; NNPDF3.1 PDFs; CMS detector simulated with Geant4.
- Pileup (PU) included; events weighted to match data (avg. PU: 23, 33, 32 respectively for 2016–2018).

Selections and expected yields

Table: Summary of the event selections. The aQGC SR requires additionally $p_{\mathrm{T}}^{\gamma} > 60$ GeV.

Region	N_ℓ [GeV]	N_γ [GeV]	N_{OSSF} [GeV]	$N_{b\text{-tag}}$ [GeV]	$p_{\mathrm{T}}^{\mathrm{miss}}$ [GeV]	p_{T}^{ℓ} [GeV]	$\min(m_{\ell\ell})$ [GeV]	$\lvert m_{\ell_{Z1}\ell_{Z2}} - m_Z \rvert$ [GeV]	$m_{\ell_{Z1}\ell_{Z2}\ell_W}$ [GeV]	$m_{\ell_W\gamma}$ [GeV]
SR	$= 3$	≥ 1	≥ 1	$= 0$	> 30	$> \{25, 15, 25, -\}$	> 4	< 15	> 100	< 75 or > 105
ZZ CR	$= 4$	N/A	≥ 1	$= 0$	< 30	$> \{25, 15, 25, 15\}$	> 4	< 15	> 100	N/A
Nonprompt lepton CR	$= 3$	N/A	≥ 1	> 0	> 30	$> \{25, 15, 25, -\}$	> 4	> 15	> 100	N/A
Nonprompt photon CR	$= 2$	≥ 1	$= 1$	> 0	< 30	$> \{25, 15, -, -\}$	> 4	> 15	N/A	N/A

Table: Number of events in data and predictions after the combined fit for the relevant processes in the SR and CRs. All analysis uncertainties are included.

Process	SR	Nonprompt lepton CR	Nonprompt photon CR	ZZ CR
$WZ\gamma$ signal	60.8 ± 3.5	0.66 ± 0.09	0.20 ± 0.04	0.017 ± 0.008
VV	12.99 ± 0.32	1.86 ± 0.12	0.164 ± 0.017	1016 ± 12
$V\gamma$	1.8 ± 0.9	4.7 ± 2.1	438 ± 27	0.011 ± 0.006
VVV	1.6 ± 0.4	0.36 ± 0.11	0.011 ± 0.007	0.10 ± 0.04
Top	3.3 ± 0.6	227 ± 15	27.0 ± 5.9	0.30 ± 0.04
Nonprompt lepton	12.9 ± 2.8	1792 ± 34	< 0.01	< 0.01
Nonprompt photon	15.8 ± 2.2	< 0.01	195 ± 19	< 0.01
Total prediction	109 ± 5	2027 ± 33	660 ± 21	1016 ± 12
Observed	108	2029	658	1017

Measurement of $WZ\gamma$ production

- $WZ\gamma$ signal extracted via a simultaneous binned likelihood fit in SR and CRs.
- Fits use $m_{Z\gamma}$ and $m_{\ell\ell\ell}$ distributions to constrain backgrounds.
- $WZ\gamma$ and ZZ normalizations float; nonprompt backgrounds fixed from data.
- Systematic uncertainties included as nuisance parameters.
- Measured signal strength $\mu = 1.47 \pm 0.31$ with observed (expected) significance of $5.4\ (3.8)\,\sigma$.

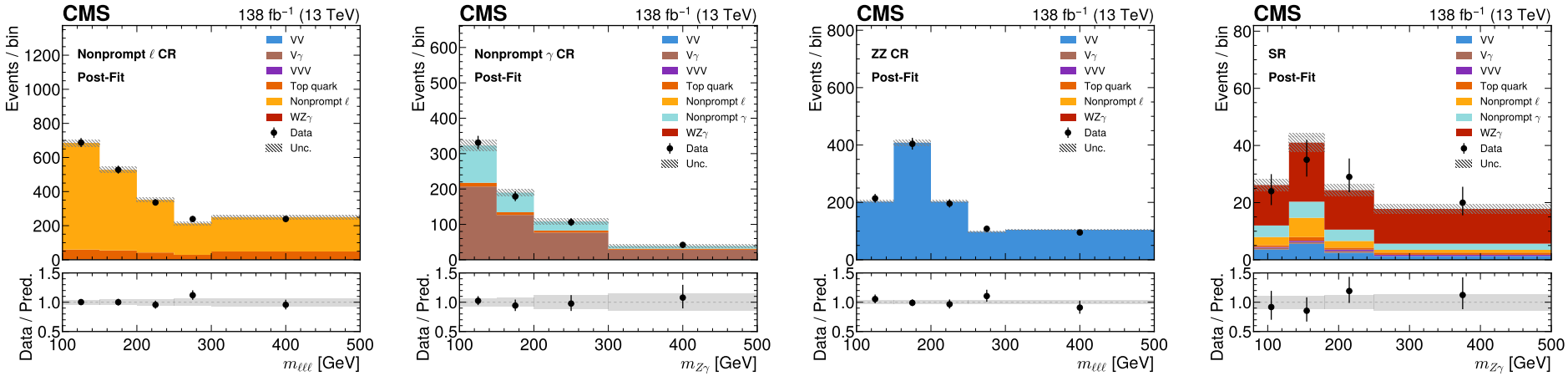

Figure: Distributions used in the simultaneous fit. Overflow events are included in the last bin.

Fiducial Cross Section and aQGC Limits

Fiducial Cross Section:

- Emulating the reco-level selection in a particle-level phase space.
- Using dressed leptons, absorbing FSR photons with $\Delta R(\ell, \gamma) < 0.1$.
- Extracted with the same fit strategy as the signal measurement; non-fiducial SR events treated as background.
- Measured cross section $\sigma_{\text{fid}}^{\text{obs}} = 5.48 \pm 1.11$ pb, compatible with the SM prediction.

aQGC Limits:

- aQGCs probed using dimension-8 EFT operators affecting $WZ\gamma$ production.
- Sensitivity driven by the high-mass tail of the $m_{\ell\ell\ell\gamma}$ distribution.
- Limits obtained from a profile likelihood fit, varying one operator at a time.
- No deviation from the SM observed; 95% C.L. limits set (detailed in Slide 20), consistent with other measurements.

Limits on photophobic ALP models

- Photophobic axion-like particle (ALP) models are probed assuming $a \to Z\gamma$.
- The invariant mass $m_{\ell_{Z1}\ell_{Z2}\gamma}$ is used as the discriminating observable.
- The SM $WZ\gamma$ process is treated as background, constrained in a simultaneous fit.
- No significant excess observed; 95% C.L. upper limits are set using the $\mathrm{CL_s}$ method.
- Limits are placed on the ALP coupling parameter $1/f_a$ as a function of the ALP mass, providing new (110–200 GeV) and competitive (200–400 GeV) constraints.

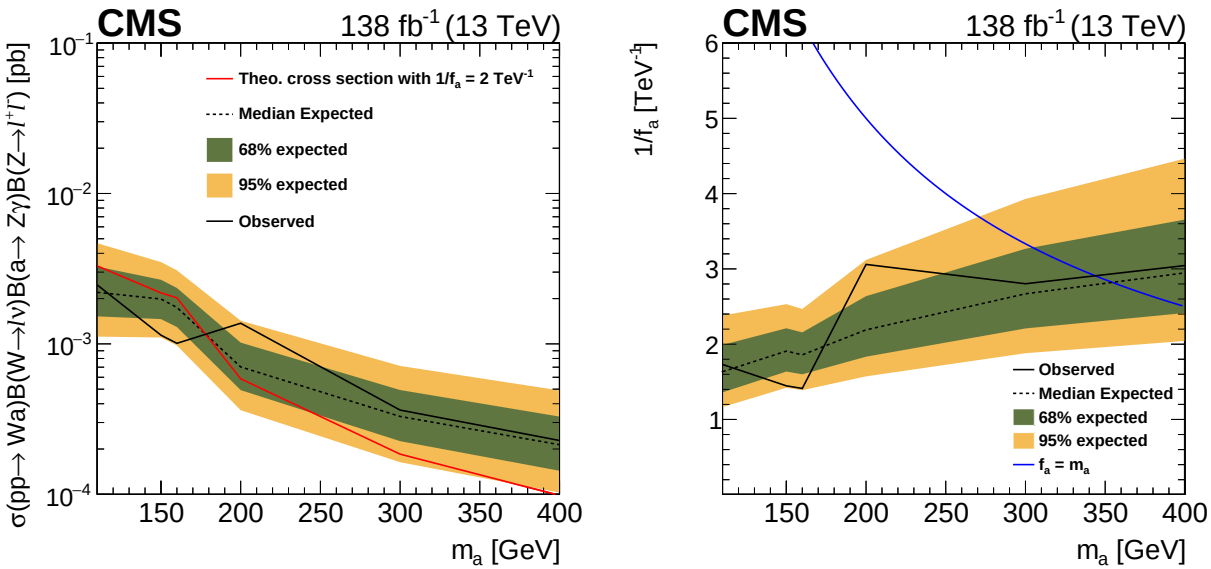

Figure: Expected and observed 95% C.L. upper limits. The red curve shows the prediction for $1/f_a = 2\ \mathrm{TeV}^{-1}$, and the blue line indicates the EFT validity boundary $m_a = f_a$.

Summary

Summary

Beyond new particles, precise tests of the SM can reveal new physics through *subtle deviations in polarization and rare multi-boson processes*.

$H \to ZZ^*$ polarization measurement:

- $\sqrt{s} = 13$–$13.6\ \mathrm{TeV}$ on CMS Run-II and early Run-III data $(200\ \mathrm{fb}^{-1})$
- Polarization fractions $f_L = 0.49^{+0.08}_{-0.07}$, $f_\perp = 0.25^{+0.21}_{-0.22}$
- Observed $f_L \neq 1$ $(> 5\,\sigma) \Rightarrow$ observation of quantum entanglement
- Results fairly consistent with SM expectations, interpreted as EFT constraints

$WZ\gamma$ observation:

- $\sqrt{s} = 13\ \mathrm{TeV}$ on CMS Run-II data $(138\ \mathrm{fb}^{-1})$
- Observed (expected) significance: $5.4\ (3.8)\,\sigma$
- Fiducial cross section: $5.48 \pm 1.11\ \mathrm{fb}$ (agrees with NLO prediction: $3.69 \pm 0.24\ \mathrm{fb}$)
- Comparable limits on aQGCs and new constrains on massive ALP production

Thanks for your attention!

Backup

$H \to ZZ^*$ polarization modeling

Mass-independent modeling (this talk):

- The mass distribution is assumed to be invariant across polarization modes.
- Analytical morphing of a_i is applied to keep the mass distribution unchanged under reweighting.
- A mass-ignorant fitting strategy is pursued, yielding a more conservative approach.

Mass-dependent modeling (complementary alternative):

- Changes in the mass distribution from SM to LL/TT are determined by the SM.
- For LL (TT) reweighting, helicity amplitudes are set such that $A_{\pm\pm} = 0$ ($A_{00} = 0$) and A_{00} ($A_{\pm\pm}$) take their SM values on an event-by-event basis.
- Following Refs. Aguilar-Saavedra *et al.*, PRD 107 (2023) 016012, Maina *et al.*, EPJC 81 (2021) 989, and Maina *et al.*, PLB 820 (2021) 136360.

Object reconstruction and event selection

Object reconstruction:

- Muons: $|\eta| < 2.5$, $p_{\mathrm{T}} > 15$ GeV, tight/loose/veto working points; $\Delta R = 0.4$.
- Electrons: $|\eta| < 2.5$, $p_{\mathrm{T}} > 15$ GeV; tight/loose/veto IDs; supercluster for bremsstrahlung recovery; isolation via effective area.
- Photons: $|\eta| < 2.5$, $p_{\mathrm{T}} > 20$ GeV; tight/loose IDs.
- Jets: PF objects clustered with anti-k_T $R = 0.4$, pileup mitigation; b-tagging with DeepCSV tight WP.

Event selection:

- Exactly 3 tight leptons: 2 OSSF for Z ($p_{\mathrm{T}} > 25, 15$ GeV), 1 for W ($p_{\mathrm{T}} > 25$ GeV).
- ≥ 1 tight photon ($p_{\mathrm{T}} > 20$ GeV); $m_{\ell\ell\ell} > 100$ GeV; $m_{\ell\ell} > 4$ GeV.
- $p_{\mathrm{T}}^{\mathrm{miss}} > 30$ GeV; b-jet veto; 4$^{\mathrm{th}}$ lepton veto.
- $m_{\gamma e_W}$ outside (75,105) GeV to suppress $Z + \gamma$.
- aQGC SR: same as SR, $p_{\mathrm{T}}^{\gamma} > 60$ GeV.
- Control regions: nonprompt ℓ CR, nonprompt γ CR, ZZ CR.

Background estimation

- Dominant backgrounds: nonprompt photons, nonprompt leptons, and ZZ production.
- Nonprompt objects:
  - Arise from misidentified jets/leptons, often during parton shower/hadronization.
  - Estimated from data due to poor modeling in simulation.
- ZZ background:
  - Comes from $e \to \gamma$ misidentification or leptons outside acceptance/ID.
  - Estimated from simulation and constrained via CR.
- Nonprompt photons:
  - Mainly from WZ+jets or tZ+jets with jets faking photons.
  - Estimated using per-event extrapolation factors from data based on $\sigma_{i\eta i\eta}$ template fits.
- Nonprompt leptons:
  - Mainly from ttZ, ttW, and jet-enriched processes.
  - Estimated similarly to photons; τ-decay leptons from simulation.
  - Misidentification rate f_l measured in dijet-enriched region and applied to loose-but-not-tight leptons.
- Other backgrounds (top quark, multiboson) from MC simulation, normalized to theoretical cross sections; overlaps removed.

aQGC Limits

Table: Exclusion limits at the 95% C.L. for each aQGC coefficient, assuming all other coefficients are set to zero. Unitarity bounds corresponding to each operator are also listed.

Operators	Observed limits $[\mathrm{TeV}^{-1}]$	Expected limits $[\mathrm{TeV}^{-1}]$	Unitarity bound $[\mathrm{TeV}^{-1}]$
$F_{\mathrm{T},0}/\Lambda^4$	$[-2.60, 2.60]$	$[-2.52, 2.52]$	1.32
$F_{\mathrm{T},1}/\Lambda^4$	$[-3.28, 3.24]$	$[-3.18, 3.14]$	1.48
$F_{\mathrm{T},2}/\Lambda^4$	$[-7.15, 7.05]$	$[-6.95, 6.85]$	1.35
$F_{\mathrm{T},5}/\Lambda^4$	$[-2.54, 2.56]$	$[-2.46, 2.50]$	1.55
$F_{\mathrm{T},6}/\Lambda^4$	$[-3.18, 3.22]$	$[-3.08, 3.14]$	1.61
$F_{\mathrm{T},7}/\Lambda^4$	$[-6.85, 7.05]$	$[-6.65, 6.85]$	1.71